

The application of EBSD analysis to biomaterials: microstructural and crystallographic texture variations in marine carbonate shells

/ Erika Griesshaber (1) / Rolf D. Neuser (2) / Wolfgang W. Schmahl (1)

(1) Department für Geo- und Umweltwissenschaften, Ludwig Maximilians Universität, Theresienstraße 41, D-80333 München, Germany.

(2) Institut für Geologie, Mineralogie und Geophysik, Ruhr-Universität-Bochum, Universitätsstraße 150, 44801 Bochum, Germany.

Abstract

Electron backscatter diffraction (EBSD) is a facile and highly automatized microdiffraction method suitable for the determination of crystallographic phase and crystallite orientation. Thus, EBSD is an ideal method for the investigation of the structural organization of materials. Mineralized structures generated by biological control are widely recognized as prototypes for advanced materials. Their advanced properties are obtained through the interlinkage of two distinct material components - mineral and biopolymer - and by the development of highly evolved microstructures. We study the hierarchical structural organization of calcium carbonate skeletons of marine organisms as well as the interlinkage of the organic and inorganic components within these biomaterials. Our investigations range over several hierarchical length scales. In this paper we discuss as an example the microstructural and textural features of the calcitic shell of the brachiopod *Notosaria nigricans*. Furthermore, we address specific textural features of brachiopod calcite biomineralization in the course of shell growth. Based on the size and morphology of calcite crystals the shell of *Notosaria nigricans* is structured into two main layers which each consist again of sublayers. The primary layer on the outside of the shell shows an outer sublayer composed of nanosized crystallites and an inner sublayer with micrometre sized crystallites. The primary layer is followed inward by a secondary shell layer composed of fibrous calcite crystals. Sublayers of the secondary layer are distinguished by an alternation of domains where the morphological axis of the calcite fibres run in different directions in the plane parallel (or up to 10° inclined) to the shell surface. While in the juvenile brachiopod we have only three sublayers with distinctly oriented fibres in the secondary layer, the adult brachiopod shows several sublayers. The preferred crystallographic orientation of both the primary and the secondary shell layers is a strong fibre texture. Calcite c-axes are perpendicular (up to 22° subperpendicular) to the shell vault and rotate with the curvature of the shell. Accordingly, the calcite c-axis is perpendicular and mostly perpendicular to the morphological fibre axis. In juvenile as well as in adult *Notosaria nigricans* there is a slight inclination in c-axis orientation between the shell sublayers. It is remarkable that in juvenile *Notosaria nigricans* a true three dimensional crystallographic preferred orientation is present in the shell, while at a later stage of growth, in adult *Notosaria nigricans*, the texture loses most of its 3D ordering and becomes a 1D fibre texture. At the hinge of brachiopods shells restructuring is needed during growth, and here the texture becomes bi- or even multimodal.

Key-words: EBSD, Texture, Microstructure, 3D Crystallographic Preferred Orientation, Biomineralization of Modern Brachiopod Shells, Nacre, Hybrid Composite Material, Biomaterial Architecture

1. Introduction

Electron backscatter diffraction (EBSD) is a microdiffraction method which is currently evolving rapidly (*Schmidt & Olesen, 1989; Dingley, 2004; Deal & Hoogan, 2008; Zaefferer et al., 2008*). EBSD provides space-resolved information on the phase state of the material and on the crystallite orientation with a precision in the order of 0.3°. The spatial resolution depends on the system and the sample in question, and it is currently in the order of 1 µm for carbonates and 100 nm or better for metals. The accuracy of lattice parameter measurement, however, is currently only in the order of 0.1% -1%.

Mineralized structures generated by biological control are widely recognized in materials science and nanotechnology as prototypes for advanced materials. The scientific interest in biomaterials, composite materials, nanostructures and biomimetic processes has focused considerable efforts in the investigation of textural, microstructural and mechanical properties of mollusc shells (*Currey & Taylor, 1974; Jackson et al., 1988; Sarikaya & Aksay, 1995; Kamat et al., 2000; Okumara & de Gennes, 2001; Mayer & Sarikaya, 2002; Song & Bai, 2002; Li et al., 2004; Katti et al., 2005; Gao, 2006; Barthelat & Espinosa, 2007; Currey, 1977*). Currey and coworkers (*Currey & Taylor, 1974; Currey, 1977*) described and investigated mollusc nacre, a natural hybrid nanocomposite that is an assemblage of nanoscale aragonite platelets in an organic matrix. It has been proven that mollusc nacre has superb mechanical properties, e.g. its fracture toughness is increased by two to three orders of magnitude relative to the purely inorganic mineral component (*Currey & Taylor, 1974; Currey, 1977; Jackson et al., 1988; Sarikaya & Aksay, 1995; Kamat et al., 2000; Okumara & de Gennes, 2001; Mayer & Sarikaya, 2002; Song & Bai, 2002; Li et al., 2004; Katti et al., 2005; Gao, 2006; Barthelat & Espinosa, 2007*). The key features for the optimization of mechanical performance beyond the fundamental base-parameters of the mineral or polymer components are the microstructure and the texture. In this context it is of great importance to investigate the design princi-

ples of shells of other phyla, especially of those which were very successful and abundant throughout almost the entire geological record, starting early in the history of evolution of life. Brachiopods are an ancient phylum of shell forming sessile marine invertebrates. They have existed in a wide variety of habitats since the early Cambrian and therefore present us with an immense fossil record of marine facies in space and time. Brachiopods were among the pioneering phylae to develop all three of the main chemical groups of exo- and endoskeleton biomaterials (*Lowenstam, 1981*): calciumcarbonate (in the subphylae *Craniformea* and *Rhynchonelliformea*) and organocalciumphosphates (in the *Linguliformea*) and even silica which has been observed in larval linguliform brachiopods by *Williams et al. (1998)*. The key features of the materials design for both groups of brachiopod shells are that both are hybrid composite materials and have a hierarchical architecture. The ability of the calcitic subphylae to produce stable, more or less diagenesis-resistant low-Mg calcite shells and their ubiquitous distribution in marine environments renders them as key objects not only for evolutionary but also for paleoclimatic and paleo-oceanographic studies (*Grossmann et al., 1996; Veizer et al., 1999; Brand et al., 2003*). However, the interpretation of isotopic signals from brachiopod shells relies on the knowledge of species- and metabolic-related differences in C- and O-isotope fractionation between the ambient sea water and the calcite precipitating under physiologic control (*Rush & Chafetz, 1990; Carpenter & Lohmann, 1992 and 1995; Samtleben et al., 2001; Buening, 2001; Curry & Fallick, 2002; Auclair et al., 2003; Weiner & Dove, 2003; Parkinson et al., 2005; Griesshaber et al., 2007*).

Our previous work on the microstructure and the texture of specimens of the modern terebratulide brachiopod species *Megerlia truncata* and *Terebratalia transversa* (*Griesshaber et al., 2007; Schmahl et al., 2004; Griesshaber et al., 2005a and b*) revealed that terebratulide brachiopod shells usually consist of a thin, outer, hard, protective layer composed of nanocrystalline calcite that is bordered inwardly by a thicker and distinctly softer,

secondary layer build of stacks of long calcite fibres (for a detailed description see Griesshaber et al. (2007); Schmahl et al. (2008)). The valves of these shells have a strong fibre texture, while within the hinge region a bimodal or multimodal c-axis distribution pattern prevails. Furthermore, our previous investigations have shown that different microstructural features exist not only for the dorsal and the ventral valves but also for the anterior and posterior parts of the shell. We can infer from these textural observations that during shell formation several distinct metabolic environments prevailed at different parts of the shell and created the high functional specialization of the different shell portions and thus induced a pronounced scatter of stable-isotope results within the same shell (e.g. Carpenter & Lohmann, 1992; Samtleben et al., 2001; Buening, 2001; Parkinson et al., 2005). In this paper we present an ontogenetic study of the shell microstructure and texture of the modern rhynchonellide brachiopod species *Notosaria nigricans*. For this purpose

we have chosen juvenile (2 mm in length), adolescent (9 mm in length) and adult forms (1.8 cm) from the same locality and have tracked the presence and investigated the development of microstructural and textural features in the shell of distinctly aged specimen of *Notosaria nigricans*.

2. Materials and methods

In electron backscatter diffraction (EBSD) the monochromatic electron beam of a scanning electron microscope (SEM) is directed onto a surface point of the sample at an angle of 30° with respect to the sample surface (Figs. 1a, 1b). The electron beam creates a point source of electrons where it hits the sample surface. A Kikuchi-diffractogram (Fig. 1c) emerges from this point source in the proximity of the surface as the electrons radiating out are diffracted by all lattice planes of the specimen. The diffractogram is recorded on a CCD-detector at 90° to the incoming beam. The diffraction pattern is indexed automatically in order to obtain the

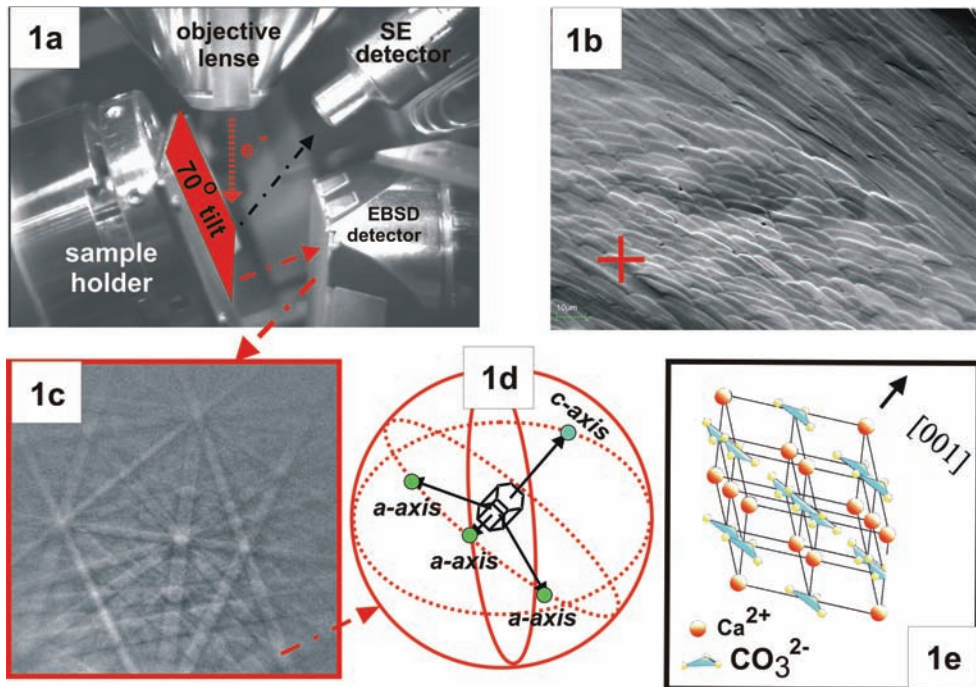


fig. 1. Principle of Electron Backscatter Diffraction. The electron beam of an SEM (a) is directed to one point on the polished surface of a sample at an angle of 30° to the surface (b). Diffraction of electrons emerging in all directions from this point occurs at the lattice planes on the sample surface. The resulting Kikuchi diffraction pattern (c) is recorded with a CCD detector at 90° to the incoming beam. Indexing of the Kikuchi diffraction pattern gives lattice information: crystallite orientation (d) and mineral phase (e).

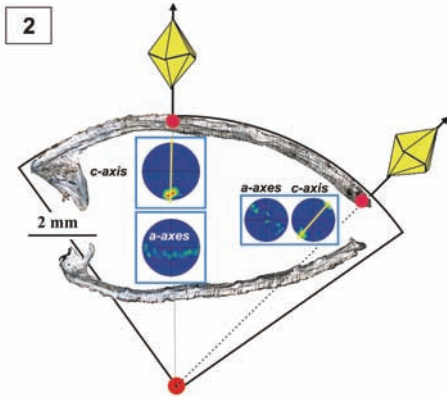


fig. 2. Two EBSD data sets visualizing calcite crystal orientation at two different parts of the valve as well as the rotation of calcite c-axis with the curvature of the valve.

crystallite phase and orientation at the point where the electron beam hits the sample (Fig.1 and Schmidt & Olesen (1989)). The experiment can be conducted either at one specific point of the sample (Fig. 1b) or at a multitude of points (Fig. 2) by step-scanning the beam or the sam-

ple. The scanning experiment yields an orientation map (Figs. 3a, 3b). EBSD data sets are displayed as band contrast (Fig. 3a) and orientation maps (Fig. 3b). Band contrast is the average intensity of the Kikuchi bands compared to the overall intensity in the electron backscatter pattern. The map of band contrast produces a grey-scale image of the microstructure similar to microscopy images obtainable by backscattered electron (BSE) detectors in the SEM or reflected light microscopy. The grain boundaries show poor band contrast and thus they are outlined as dark lines in these images. In the EBSD-orientation-map (Fig. 3b) and pole figures (Fig. 3c) different colours of the data points highlight different crystal orientations within the investigated region of the sample. Crystal axes orientation (e.g. c- and a-axes for calcite) are given as pole figures, either with the individual measurement points displayed in the pole figure (colour coded for orientation, see upper pole figures in Fig. 3c) or as pole-orientation probability distribution densities within the pole figures (lower pole figures in Fig. 3d and Fig. 2).

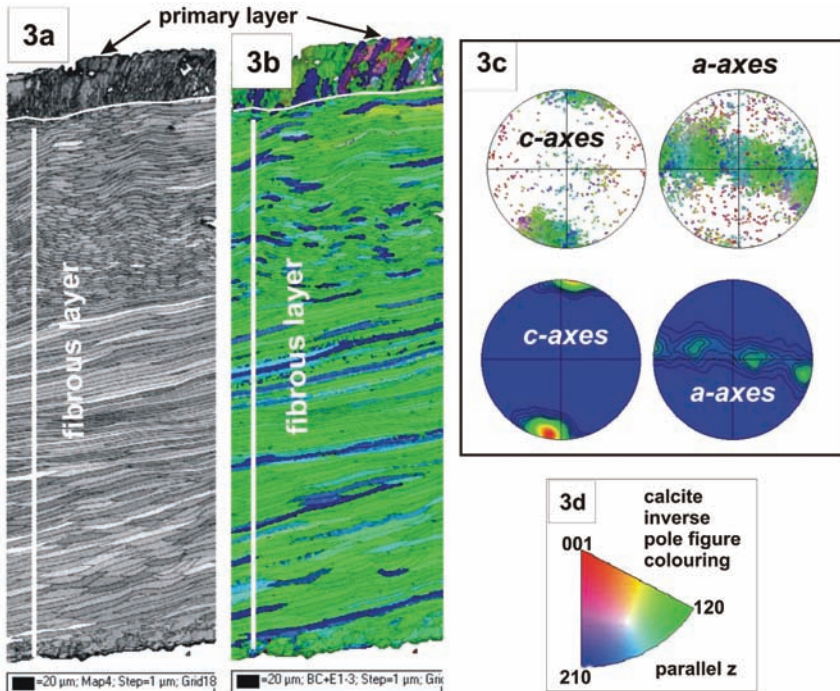


fig. 3. An EBSD data set from the central ventral valve portion. (a) band contrast image, (b) orientation map, (c) pole figures depicting individual data points colour coded as in (b) and pole density distribution; the colour code is defined in (d) as an inverse pole figure code referring to the direction of view. Well observable are the primary and the fibrous shell layers, the stacks of fibres with longitudinally and transversely cut fibres, as well as the sharp uni-axial fibre texture within this shell portion.

In this study EBSD map colouring is done with respect to inverse pole figure colours, i.e. the colour indicates the crystal axis pointing towards the viewer. The colour scheme used for all EBSD maps is given in Fig. 3d.

Specimens of different sizes (corresponding to ages) of the modern rhynchonellide brachiopod species *Notosaria nigricans* (Sowerby) were collected from shallow (from 12 to 15 m) water depth at Port Pegasus, Stewart Island, New Zealand. Sections were cut along and perpendicular to the median plane of the investigated shells and thus, 200 micrometer thick shell wafers were obtained. These were subsequently prepared on both sides as highly polished, uncovered, 150 micrometer thin sections. In order to obtain high-resolution SEM images and good EBSD patterns, the surface of the thin sections was subsequently etched for 45 seconds with a suspension of alumina nanoparticles. The samples were then cleaned, dried, and coated with the thinnest possible conducting carbon coating. Scanning electron micrographs and EBSD patterns were obtained on a LEO Gemini 1530 SEM and a JEOL JSM 6500F SEM each equipped with the HKL Technology "Channel 5" EBSD system (Schmidt & Olesen, 1989; Dingley, 2004). SEM images and EBSD patterns were generated using an accelerating voltage of 20 kV and a beam current of 3.0 nA. The lattice orientation of grains was determined with a spatial resolution of 2-3 μm and an absolute angular resolution of ± 0.5 degrees. EBSD patterns with a mean angular uncertainty of 1 degrees and above were discarded.

3. Results and discussion

Figures 4, 5 and 6 show the shell microstructure of juvenile to adult specimens of *Notosaria nigricans*. The internal structure is highlighted with orientation contrast images. Fig. 4 shows both valves at the commissural end, Fig. 5 gives two images from the central portion of the ventral valve and Fig. 6 gives a comparison between the microstructure of the valves of juvenile and adult *Notosaria nigricans*.

The shell of *Notosaria nigricans* is composed

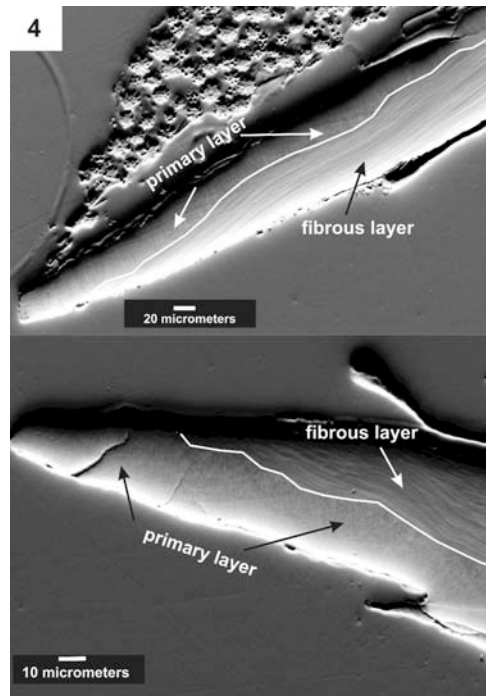


Fig. 4. Orientation contrast images of both valves of juvenile *Notosaria nigricans* at the commissural end of the shell. Well observable is the high portion of primary shell layer within the valves and the inward succession of longitudinally cut fibres.

of two distinct shell layers, an outer primary and an inner, secondary layer. While the primary layer consists of nano- to micro sized calcite crystallites, the thick inwardly located secondary layer is built of thin (~ 5 micrometers) and exceedingly long (we observed up to 500 micrometers) calcite fibres of coherent monocrystalline-like orientation. In the valve the fibres are parallel to the outer surface and slightly inclined ($\sim 10^\circ$) to the inner surface of the valve and they are stacked in parallel to form layers (Figs. 4 and 5). Sublayers of the secondary layer are distinguishable as the fibres abruptly change their morphological axis orientation by about 90 degrees (Figs. 5a, 5b). In the investigated sections through the shell, which are anterior-posterior cuts parallel to the median plane and perpendicular to the commissural opening between the ventral and dorsal shell valves, we observe the stacks of parallel fibres either sometimes as longitudinal cuts or sometimes as transverse cuts (Fig. 5b). The longitudinally sectioned fibres of the speci-

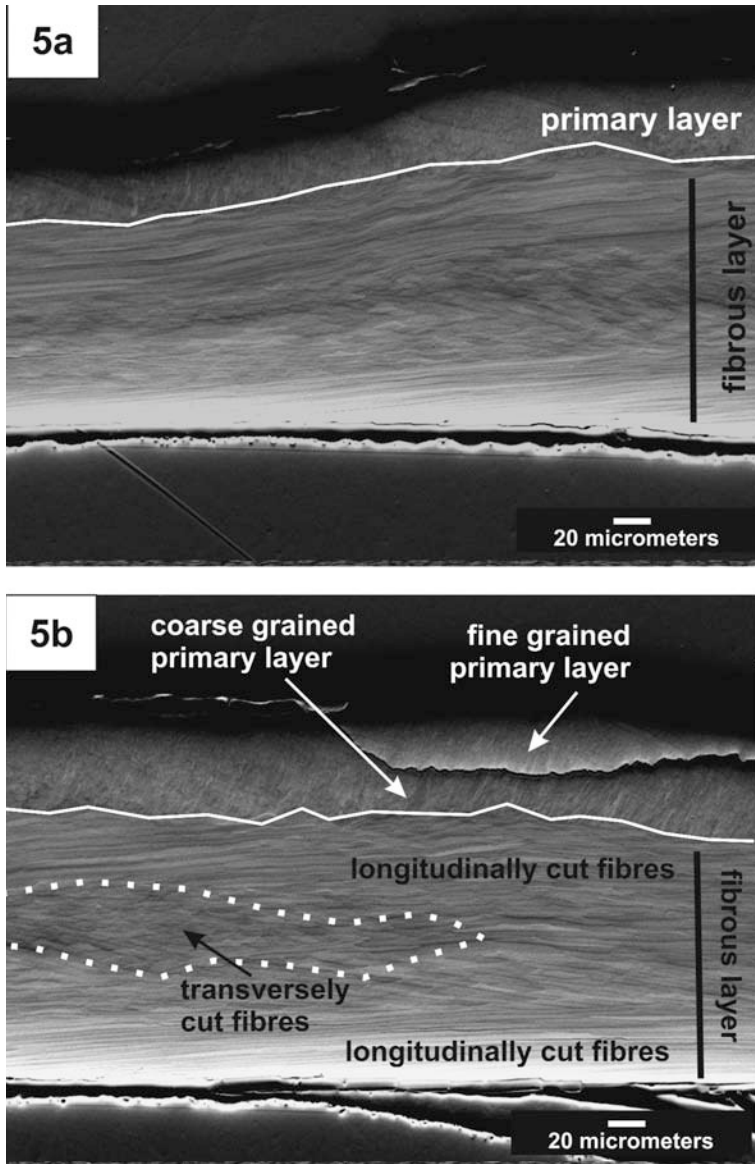


fig. 5. Orientation contrast images of the central portion of the ventral valve of juvenile *Notosaria nigricans* highlighting the two shell layers together with internal sublayers in both the primary layer and in the fibrous secondary layer.

mens are parallel to the overall direction of shell growth (*i.e.* posterior-anterior) while the cross-sectioned fibres are parallel to the commissure and perpendicular to the direction of overall shell growth. *Figs. 4 and 5* show the shell microstructure of the juvenile specimen of *Notosaria nigricans*. In the fibrous secondary layer we observe predominantly longitu-

dinally cut fibres (*Fig. 4*) and only twice the abrupt switch of fibre orientation (*Fig. 5a*), such that a single sublayer of transversely cut fibres is present between two sublayers of longitudinally cut fibres (*Fig. 5a*). This is entirely different in the adult forms. Here, in the section along the median plane of the shell we see almost predominantly transversely cut

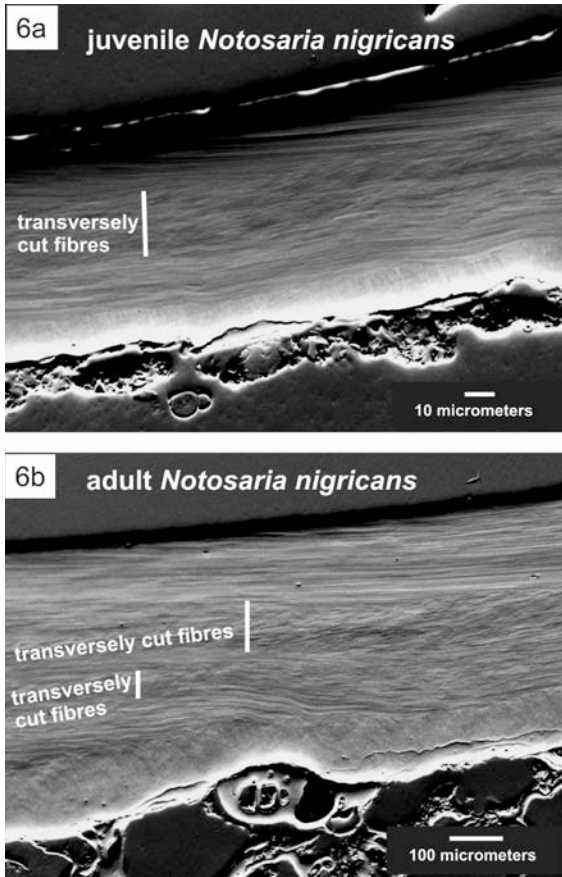


fig. 6. Orientation contrast images of the dorsal valves of juvenile (a) and adult (b) *Notosaria nigricans*. While in the juvenile specimen there are only two changes in orientation of the stacks of fibres, the adult specimen shows several orientation changes of 90 degrees. This feature resembles the plywood structure of organophosphatic biomaterials. In brachiopod shells it occurs when the animal grows and the shell gets thicker and additional shell sublayers are attached along the inward rim of the shell.

fibres and several alternations between stacks of fibres with longitudinal and transverse cuts (Fig. 6b). It should be noted, however, that for all specimens of different age, even in the adult forms, the top and the bottom of the secondary layer are generally formed by longitudinally sectioned fibres with very few local exceptions.

The primary layer of calcitic brachiopods serves as an outer protective cap (Griesshaber et al., 2007; Schmahl et al., 2008; Griesshaber et al., 2005a and b). It is the initial biomineralization product of the mantle epithelium cells before they start to produce the fibres of the

secondary layer (Williams et al, 2000). The primary layer is composed of nano- to micro-sized calcite crystals. It is also structured; in the case of *Notosaria nigricans* into two sublayers (Fig. 5b), such that along the outermost part of the shell calcite crystallites are nanosized (Figs. 4 and 5b), while towards the secondary layer they become larger and are micrometer-sized (Figs. 5a and 5b). In comparison to the adult specimen of *Notosaria nigricans* (Fig. 6b), in the juvenile animal (Fig. 4) the primary layer forms a substantial fraction of the thickness of the shell. As shown in Fig. 4 the primary layer makes up the entire tip of the valves at the commissural margin. The thickness of the shell increases with age. Accordingly, biomineralization from the mantle epithelium does not only occur at the commissural margin of the shell but also at the inner side of the shell. Mineralization of transversely oriented fibres starts about 100-200 micrometres from the commissural margin. When growth ceases episodically and growth lines form, which can be seen in Fig. 4 in the form of “horn”-like protrusions of the primary layer, the mineralization resumes at a lower and more backward position at the margin of the shell, such that the old primary layer is underplated and thickened with new material. We speculate that the production of transversely oriented material may be related to these events where the mineralizing mantle epithelium is retracted to the posterior and/or re-organized when normal growth resumes.

Figures 2, 3, 7, 8 and 9 show band contrast and orientation maps together with corresponding pole figures of juvenile and adult *Notosaria nigricans*. In order to highlight well grain sizes (predominantly in the primary shell layer) and the stacks of fibres, we superimpose band contrast images to the orientation map. To some extent band contrast images visualize the internal shell structure to a higher degree than orientation contrast images (Figs. 4, 5, 6). In almost all pole figures we observe a sharp cylindrical “fibre” texture (with the exception of the texture in Fig. 9)

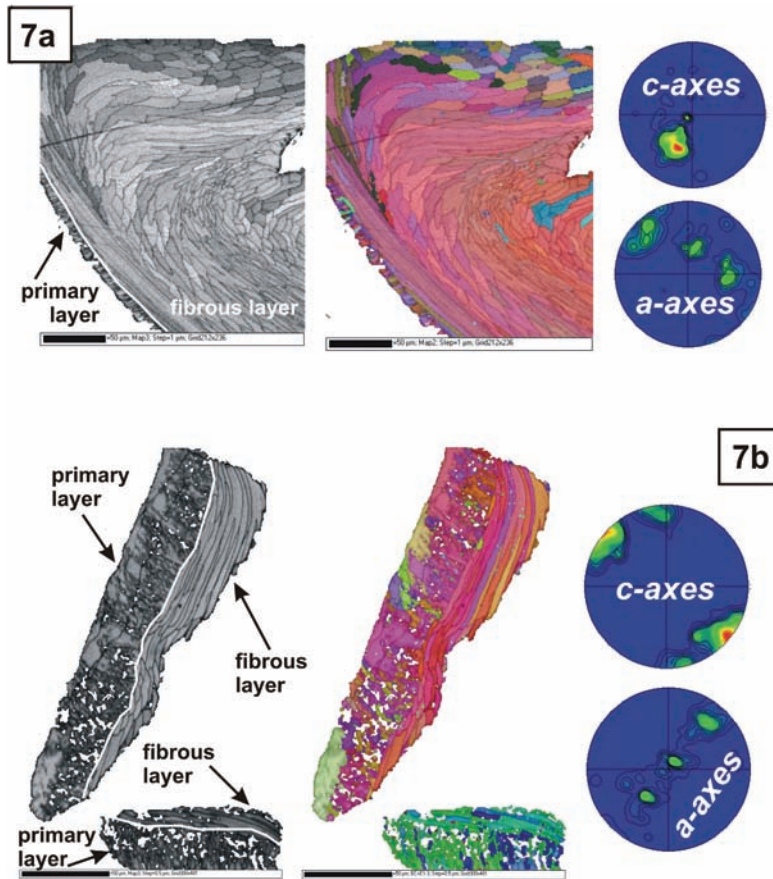


fig. 7. EBSD data sets for juvenile *Notosaria nigricans* from the hinge (a) and the commissural (b) shell portions. Gray scale image: band contrast, colour image: orientation map. Well observable are the difference in thickness of the primary layer at the hinge and at the commissure, the differentiated internal structure of the thick primary layer at the commissure and the quite sharp 3D preferred orientational patterns of calcite c- and a-axes at both shell regions.

with calcite c-axes being *perpendicular* or *sub-perpendicular* (by 22°) to the morphological fibre axes. Correspondingly the morphological fibre axes are (sub)perpendicular to the shell vault. Similar to other calcitic brachiopod species, such as *Liothyrella neozelanica*, *Liothyrella uva* (Götz et al., 2009), *Terebratalia transversa*, *Megerlia truncate* (Griesshaber et al., 2007; Schmahl et al., 2004) the direction of calcite c-axes follows the curvature of the shell, pointing radially outward (Fig. 2 for *Notosaria nigricans* and Griesshaber et al., 2007, Schmahl et al., 2004 and Götz et al., 2009). Figure 9b presents an EBSD map with the corresponding pole figure from the

hinge region of adult *Notosaria nigricans*. Even though the hinge is built of the same shell material as the valves (i.e. a nano- to microcrystalline primary layer and a fibrous secondary layer with stacks of calcite fibres in changing directions) the texture is significantly different from that of the valves. We observe a multimodal textural pattern at the hinge, confirming the similar observation for other brachiopods such as *Megerlia truncate* and *Terebratalia transversa* (Griesshaber et al., 2007).

In Fig. 9 a comparison is given between textural characteristics of the hinge of juvenile and adult *Notosaria nigricans*. This region

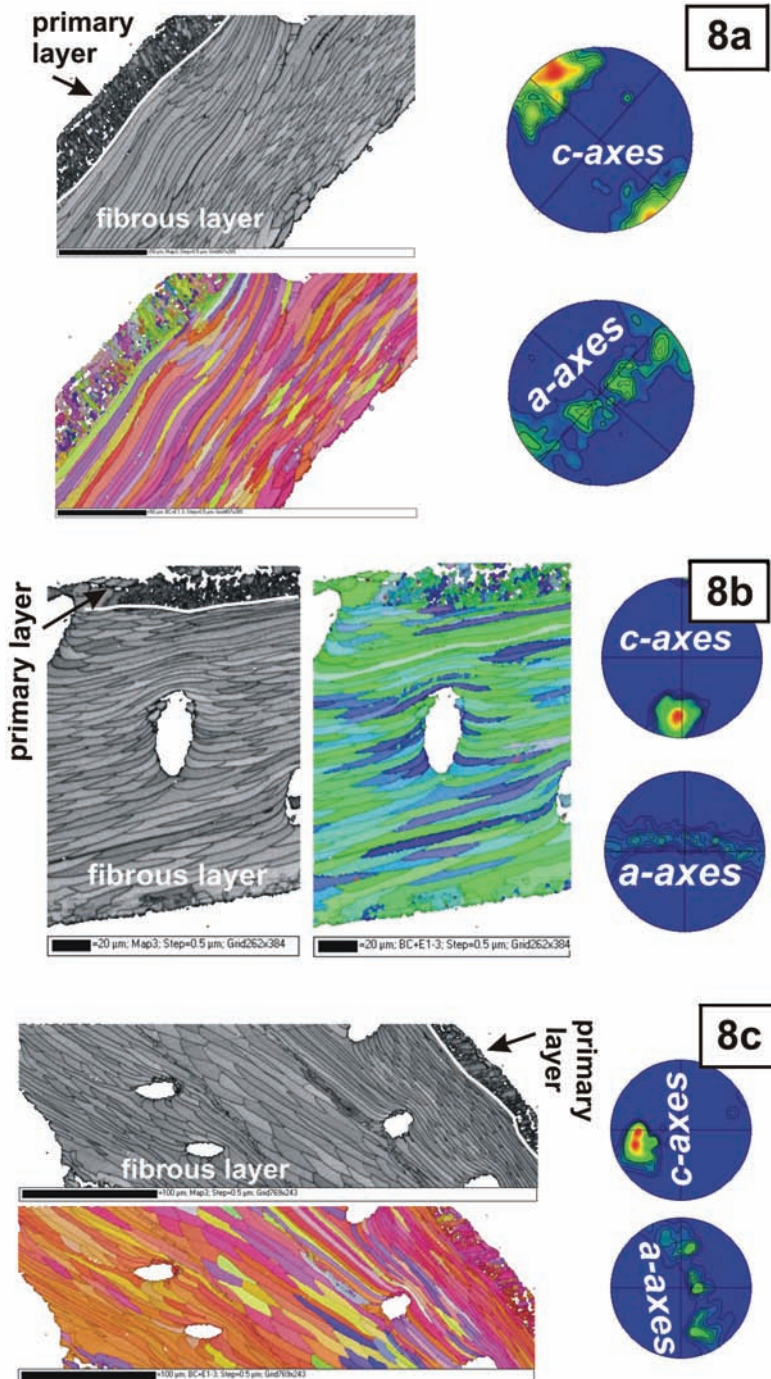


fig. 8. EBSD data sets from three distinct ventral valve portions of juvenile *Notosaria nigricans*. We can observe well the fibre texture of the valves, the rotation of the c-axis with the curvature of the shell and the sharp 3D ordering of calcite c- and a-axes.

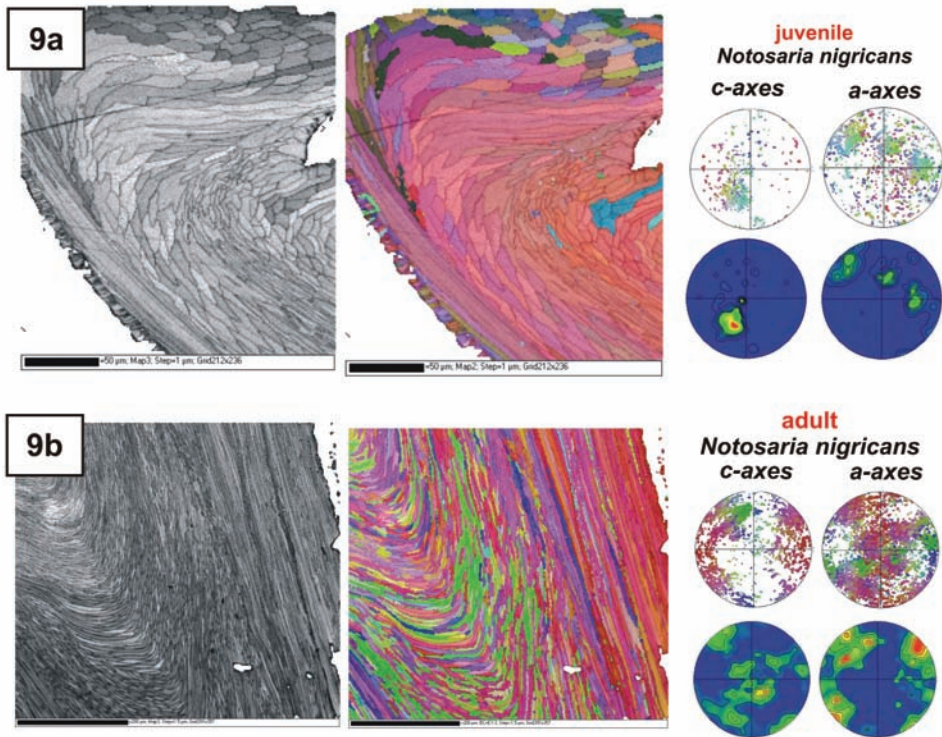


fig. 9. Comparison between the hinge of juvenile (a) and adult (b) *Notosaria nigricans*. Even though for both specimens the microstructure of the hinge and the valves is similar, we observe the following textural differences between the valves and the hinge: (i) for both specimens the texture at the hinge is less sharp in comparison to the texture of the valves. (ii) the comparison of crystallographic axes ordering between juvenile and adult specimens shows that while a high degree of 3D ordering is present in the juvenile specimen this is lost completely with growth progression and is not present any more in the adult specimen.

marks the initial parts of valve mineralization and formation. It is remarkable that in the juvenile specimen a three dimensional crystallographic preferred orientation is present as can be seen from the sharp $\{001\}$ pole and ordering of the $\{100\}$ poles into strong maxima separated by 60° corresponding to the trigonal symmetry of calcite. This is in contrast to the texture of the hinge at a later stage in growth. The texture loses 3D ordering as the $\{100\}$ poles distribute quite evenly (with cylindrical symmetry) on the great circle around the usually sharp c-axis maximum, while at the hinge the addition of more calcite material makes the texture bimodal or even multimodal.

4. Conclusions

1. Taking calcite crystal size, morphology and crystallographic orientation into considera-

tion we can deduce that the shell of *Notosaria nigricans* is highly structured. The primary layer contains two distinct sublayers: An outer layer of entirely nanosized calcite and an inner layer of predominantly micrometer-sized calcite. The fibrous secondary layer shows sublayers with alternating morphological fibre orientation which can run perpendicular or parallel to the commissure. In adult specimens the texture of both shell valve layers is a pronounced cylindrical "fibre" texture. Calcite crystal c-axes are more or less perpendicular to the morphological fibre axes and perpendicular to the shell vault. We observe a slight inclination in fibre orientation between shell sublayers with longitudinally cut fibres and transversely cut fibres. However, the fibrous calcite in the hinge of *Notosaria nigricans* does not have a unimodal texture, a multimodal distribution of c-axes prevails. The distinct microstructural and tex-

tural features of different parts of the shell suggest different regimes of physiological control of biomineralization. This conclusion is entirely in concert with conclusions of Carpenter & Lohmann (1995) and Parkinson et al. (2005) that are deduced from stable isotope distribution patterns in modern calcitic brachiopods. The authors report that in specialized parts of the shell such as the hinge, brachidium, muscle scars or the primary layer, $\delta^{18}\text{O}$ and $\delta^{13}\text{C}$ are usually depleted due to biological fractionation effects. Mechanical properties were not investigated here, but from the similarity of hierarchical microstructures to *Megerlia truncata* we expect a similar pattern of distribution of organic components in the hybrid composite (Schmahl et al., 2008; Griesshaber et al., 2009) and a similar pattern of mechanical properties (Griesshaber et al., 2005a and b; Griesshaber et al., 2007; Schmahl et al., 2008).

2. Microstructural differences are present between juvenile and adult forms of *Notosaria nigricans*. While juvenile *Notosaria nigricans* contains a high fraction of primary layer calcite, in adult *Notosaria nigricans* the shell is predominantly formed by secondary layer calcite fibres. The primary layer in the adult animals is only a thin, outer protecting cap. Further, in juvenile *Notosaria nigricans* we observe mainly calcite fibres parallel to the overall direction of growth, and only a central sublayer consists of fibres running perpendicular to the overall direction of growth. In adult *Notosaria nigricans* the shell is predominantly composed of fibres running perpendicular to the direction of growth with some interlayers of fibres running parallel to the direction of growth. Thus, in the adult forms, we find several alternations between domains of fibres growing in different directions.

3. From increasing thickness of the shell between the juvenile and the adult form it is quite evident that calcite mineralization from the mantle epithelium does not only occur at the commissural margin but also at the inner surface of the shell. In the juvenile form the shell is 50-100 micrometers thin, with the primary layer hardly exceeding 20 micrometers. As material is added later only at the inner surfa-

ce of the shell, the initially formed primary layer keeps its thickness and later forms the thin cap of the posterior part of the shell valve near the hinge. As the animal grows larger, the number of cells active in biomineralization at the anterior growth front increases, and the thickness of the deposited primary (and secondary) layer increases. Fibrous calcite material is constantly added at the inner surface of the shell, increasing its thickness, but also shaping the muscle scars and the hinge, which have to be continuously adapted to the increasing overall size of the shell. Williams et al. (2000) suggested that each calcite fibre is mineralized from a single cell of the mantle epithelium. The small ($\sim 10^\circ$) inclination angle of the fibres with respect to the inner shell surface (Figs. 1 and 2) is required for this mechanism (Williams et al., 2000).

4. The appearance of longitudinal and transverse fibre directions with respect to the overall growth direction means that the movement of the cells, as they precipitate calcite, changes direction at a particular distance (from Fig.1 it is $\sim 100\text{-}200\text{ m}$) from the margin to produce a tougher, cross-laminated microstructure. The changes in fibre direction are associated with the formation of growth steps.

Acknowledgements

We are indebted to E. Kessler, T. Westphal and D. Dettmer for the skilful preparation of samples. We would like to thank the German Research Council (DFG) for financial support.

References

- Auclair, A.C., Joachimski, M. M. & Lecuyer, C. (2003) Deciphering kinetic, metabolic and environmental controls on stable isotope fractionations between seawater and the shell of *Terebratalia transversa* (Brachiopoda). *Chem. Geol.*, 202, 59-78.
- Barthelat, F. & Espinosa, H.D. (2007) An experimental investigation of deformation and fracture of nacre-mother of pearl. *Exp. Mech.*, 47, 311-324.
- Brand, U., Logan, A., Hiller, N. & Richardson, J. (2003) Geochemistry of modern brachiopods: applications and implications for oceanography and

- paleoceanography, *Chem. Geol.*, 198, 305-334 .
- Buening, N. (2001) Brachiopod shells: Recorders of the present and keys to the past, in "Brachiopods ancient and modern; A tribute to G. Arthur Cooper", S. J. Carlson and M.R. Sandy, eds., *Pal. Soc. Pap.* 7, 117-145.
- Carpenter, S. J. & Lohmann, K.C. (1992) Sr/Mg ratios of modern marine calcite: empirical indicators of ocean chemistry and precipitation rate. *Geochim. Cosmochim. Acta*, 56, 1837- 1849.
- Carpenter, S. J. & Lohmann, K.C. (1995) $\delta^{18}\text{O}$ and $\delta^{13}\text{C}$ values of modern brachiopod shells. *Geochim. Cosmochim. Acta*, 59, 3749-3764.
- Currey, J.D. & Taylor, J.D. (1974) The mechanical behavior of some molluscan hard tissues. *J. Zool., Lond.* , 173, 395-406.
- _ (1977) Mechanical properties of mother of pearl in tension. *Proc. R.Soc. Lond. B*, 196, 443-463.
- Curry, G.B. & Fallick, A. E. (2002) Use of stable oxygen isotope determinations from brachiopod shells in paleoenvironmental reconstruction. *Palaeogeogr. Palaeoclimatol. Palaeoecol.*, 182, 133-143.
- Deal, A., Hooghan, T. & Eades, A. (2008) Energy-filtered electron backscatter diffraction. *Ultramicroscopy*, 108, 116-125.
- Dingley, D. (2004) Progressive steps in the development of electron backscatter diffraction and orientation imaging microscopy. *J. Microscopy*, 213, 214-224.
- Gao, H.J. (2006) Application of fracture mechanics concepts to hierarchical biomechanics of bone and bone-like materials. *Int. J. Fracture*, 138, 101-137.
- Götz, A., Griesshaber, E., Schmahl, W. W., Neuser, R. D., Lüter, C., Harper, E. M. & Hühner, M. (2009) The texture and hardness distribution pattern in recent brachiopods – a comparative study of *Kakanuiella chathamensis*, *Liothyrella uva* and *Liothyrella neozelanica*. *Eur. J. Mineral.* 21, 303-315.
- Griesshaber, E., Job, R., Pettke, Th. & Schmahl W.W. (2005a) Micro-scale physical and chemical heterogeneities in biogenic materials - a combined micro-Raman, chemical composition and micro-hardness investigation, in: "Mechanical properties of bio-inspired and biological materials", K. Katti, F. J. Ulm, C. Hellmich, C. Viney, eds., *MRS Symp. Proc. Ser.*, 844, 93-98.
- _ , Schmahl, W. W. , Neuser, R. D., Job, R., Bluem, M. & Brand, U. (2005b) Microstructure of brachiopod shells - an inorganic/organic fibre composite with nanocrystalline protective layer, in: "Mechanical properties of bio-inspired and biological materials", K. Katti, F. J. Ulm, C. Hellmich, C. Viney, eds., *MRS Symp. Proc. Ser.*, 844, 99-104.
- _ , _ , Neuser, R. D., Pettke, Th., Blüm, M., Mutterlose, J. & Brand, U. (2007) Crystallographic texture and microstructure of terebratulide brachiopod shell calcite: An optimized materials design with hierarchical architecture. *Amer. Mineral.*, 92, 722-734.
- _ , Kelm, K. Sehrbrock, A., Schmahl, W.W., Mader, W., Mutterlose, J. & Brand, U. (2009) Amorphous components in the shell material of the brachiopod *Megerlia truncata*, *Eur. J. Mineral.*, 21, 715-723.
- Grossmann, E. L., Mii, H.-S., Zhang, C. & Yancey, T. (1996) Chemical variation in Pennsylvanian brachiopod shells - diagenetic, taxonomic, microstructural and seasonal effects. *J. Sediment. Res.*, 66, 1011-1022.
- Jackson, A. P., Vincent, J. F. V. & Turner, R.M. (1988) The mechanical design of nacre. *Proc. R.Soc. Lond. B*, 234, 415-440.
- Kamat, S., Su, X., Ballarini, R. & Heuer, A. (2000) Structural basis for the fracture toughness of the shell of the conch *Strombus gigas*. *Nature*, 405, 1036-1040.
- Katti, K., Katti, D.R., Tang, J., Pradhan, S. & Sarikaya, M. (2005) Modeling mechanical responses in a laminated biocomposite. Part II. Nonlinear responses and nuances of nanostructure. *J. Mater. Sci.*, 40, 1749-1755.
- Li, X.D, Chang, W.C., Chao, Y.J., Wang, R.Z. & Chang, M. (2004) Nanoscale structural and mechanical characterization of a natural nanocomposite material: the shell of red abalone. *Nano Lett.*, 4, 613-617.

- Lowenstam, H.A. (1981) Minerals formed by Organisms, *Science*, 211, 1126-1131.
- Mayer, G. & Sarikaya, M. (2002) Rigid biological composite materials: Structural examples for biomimetic design. *Exp. Mech.*, 42, 395-403.
- Okumura, K. & de Gennes, P.G. (2001) Why is nacre strong? Elastic theory and fracture mechanics for biocomposites with stratified structures. *Eur. Phys. J. E*, 4, 121-127.
- Parkinson, D., Curry, G. B., Cusack, M. & Fallick, A. E. (2005) Shell structure, patterns and trends of oxygen and carbon stable isotopes in modern brachiopod shells. *Chem. Geol.*, 219, 193-235.
- Rush, F. P. & Chafetz, H. S. (1990) Fabric-retentive, non-luminescent brachiopods as indicators of original $\delta^{13}\text{C}$ and $\delta^{18}\text{O}$ composition: A test. *J. Sediment. Petrol.*, 60, 968-981.
- Samtleben, C., Munnecke, A., & Bickert, T. (2001) Shell succession, assemblage and species dependent effects on the C/O- isotopic composition of brachiopods - examples from the Silurian of Gotland. *Chem. Geol.*, 175, 61-107.
- Sarikaya, M. & Aksay, I.A. (eds, 1995) *Biomimetics, design and processing of materials*. Woodbury, New York.
- Schmahl, W. W., Griesshaber, E., Neuser, R. D., Lenze, A., Job, R. & Brand, U. (2004) The microstructure of the fibrous layer of terebratulide brachiopod shell calcite. *Eur. J. Mineral.*, 16, 693-697.
- _, _, _, Merkel, C., Deuschle, J., Götz, A., Kelm, K., Mader, W. & Sehrbrock, A. (2008) Crystal morphology and hybrid fibre composite architecture of phosphatic and calcitic brachiopod shell materials - an overview. *Mineral. Mag.*, 72, 541-562.
- Schmidt, N.H. & Olesen, N.O. (1989) Computer-aided determination of crystal-lattice orientation from electron channeling patterns in the SEM. *Can. Mineral.*, 27, 15-22.
- Song, E. & Bai, Y. (2002) Nanostructure of nacre and its mechanical effects. *Int. J. Nonlin. Sci. Num.*, 3, 257-260.
- Veizer, J., Ala, D. & Azmy K. (1999) $^{87}\text{Sr}/^{86}\text{Sr}$, $\delta^{13}\text{C}$ and $\delta^{18}\text{O}$ evolution of Phanerozoic seawater, *Chem. Geol.*, 161, 59-88.
- Weiner, S. & Dove, P. M. (2003) An overview of biomineralization processes and the problem of vital effect. *Rev. Mineral. Geochem.*, 54, 1-31.
- Williams, A., Cusack, M., Buckman, J. & Stachel, T. (1998) Siliceous tablets in the larval shells of apatitic discinid brachiopods. *Science*, 279, 2094-2096.
- _, Carlson, S.J. & Brunton, C.H.C (2000) Brachiopod classification, in Williams, A. et al. *Brachiopoda (revised)*, Treatise on Invertebrate Paleontology (Kaesler, R.L., ed.). Boulder, Colorado: Geological Society of America and Lawrence, Kansas: The University of Kansas, ISBN 0-8137-3108-9.
- Zaefferer, S., Wright, S. I. & Raabe, D. (2008) Three-dimensional orientation microscopy in a focussed ion beam - scanning electron microscope: A new dimension of microstructure characterization. *Metall. Mater. Trans. A*, 39A, 374-389.